Check for updates

Impact of climate change on hydro-climatological parameters in North Cyprus: application of artificial intelligence-based statistical downscaling models

Gozen Elkiran [iD] [a,*], Vahid Nourani [a,b], Ogodor Elvis [a] and Jazuli Abdullahi [iD] [c]

[a] Near East University, Faculty of Civil and Environmental Engineering, Near East Boulevard, 99138, Nicosia, North Cyprus
[b] Center of Excellence in Hydroinformatics and Faculty of Civil Engineering, University of Tabriz, Tabriz, Iran
[c] Department of Civil Engineering, Faculty of Engineering, Baze University, Abuja, Nigeria
*Corresponding author. E-mail: gozen.elkiran@neu.edu.tr

[iD] GE, 0000-0001-5632-1856; JA, 0000-0002-2971-4475

ABSTRACT

There are many environmental challenges in water-limited places in the 21st century, particularly in dry and semi-arid regions, due to the threat of climate change caused by the greenhouse effect. This study intends to explore and assess the influence of climate change on hydro-climatological parameters using statistical downscaling and future forecasts of mean monthly precipitation and temperature through-out Famagusta (Mağusa), Nicosia (Lefkoşa), and Kyrenia (Girne) stations, North Cyprus. To achieve the study's goal, 13 predictors of BNU-ESM GCMs from CMIP5 were used at a grid point in the Karfas region. To find the primary predictors, GCM data were screened using mutual infor-mation (MI) and correlation coefficient (CC) feature extraction methods prior to downscaling modeling. A neural network (ANN), an adaptive neuro fuzzy inference system (ANFIS), and multiple linear regression (MLR) models were employed as the downscaling models. We used the best downscaling model as a benchmark for future precipitation and temperature estimates for the period 2018–2040 under the RCP4.5 scen-ario. In the future, Famagusta and Nicosia would have up to 22% less rain, and Famagusta and Kyrenia will have 2.9% greater heat. The findings of this research could be useful in decision-making, as well as water resource management and climate change.

Key words: global circulation models, precipitation, predictors, statistical downscaling, temperature

HIGHLIGHTS

- The paper use the downscaling modeling for parameter evaluation.
- It reveals the temperature and rainfall variation for future prediction, 2045.
- It analyses the effective parameter/s used for present and future evaluation.
- It is a good reference source for researchers dealing with the topic.

1. INTRODUCTION

Water resources and many other life aspects are affected by the global change of climate in many developing and developed countries around the world (Alotaibi *et al.* 2018). Over the recent decades, research on climate change has achieved tremen-dous significance due to global warming. In several parts of the globe, the variations in rainfall and temperature differs owing to the consequence of climate changes (Peng *et al.* 2018).

The general circulation models (GCMs) are used to study the future fluctuations of temperature and precipitation in such a way, that up to the end of the century, large-scale climate data are simulated under the greenhouse gas changes effect. In the local climate studies, the developed GCM outputs in coarse spatial resolution cannot directly be used. As a result, suitable techniques should be used to downscale the coarse spatial resolution of GCM outputs into finer local climate data (Mora *et al.* 2014). The downscaling models are generally classified into: (a) dynamical downscaling method that uses regional cli-mate models (RCMs) based on boundary condition set by GCM data to extract local scale information and (b) statistical downscaling method which is based on creating statistical relationship between the predictand (local scale weather data) and predictors (large-scale climate variables). The methods used for statistical downscaling are simple to use and require little efforts for computations and can be applied in different regions for different GCM outputs (Timbal *et al.* 2003).

Many methods of statistical downscaling can be found in the literature, including statistical downscaling model (SDSM) (Samadi *et al.* 2013a, 2013b), correlation analysis (Landman *et al.* 2001), multiple linear regression (MLR) (Klein 1983), the nearest neighborhood (Zorita & Von Storch 1999), adaptive neuro fuzzy inference system (ANFIS) (Alotaibi *et al.* 2018), and artificial neural network (ANN) (Nourani *et al.* 2018) among others, which have already been used to downscale statistically the GCM outputs.

Focusing on the survey of literature on the consequence results achieved for statistical downscaling modeling of climatic parameters based on the application of AI-based methods, e.g., ANNs, it was found that there are contradicting issues regarding their performance; while some studies show efficiency and superiority of ANNs, others demonstrate inferiority and drawback of ANNs over MLR-based models (e.g., Abdellatif *et al.* 2013). The quantity and quality of the used data may contribute to the inconsistency of these results. AI-based modeling challenging issues for huge amounts of data arise from noise presence in the data set and redundant information. While using the nonlinear models (such as ANN and ANFIS), over the simulation time, the noise present in the data set can be nonlinearly magnified. According to a study by Bowden *et al.* (2005), in ANN-based hydro-climatic processes modeling, utilization of several input variables may lead to inefficient results owing to: (i) irrelevant input variables, which lead to difficulty in training process; (ii) lack of convergence and low precision can be caused by the irrelevant input variables; (iii) being more time-consuming and an increase in computational memory; and (iv) it is more difficult to understand the complex models formed using huge inputs in comparison to simple models, more especially when the results of the models are compared. As such, the AI-based downscaling models' efficiency can be largely enhanced by input feature extraction methods as a preprocessing technique.

Some studies, such as Babel *et al.* (2017), utilized data preprocessing techniques in addressing the complexity in statistical downscaling modeling of GCM data through extraction of dominant predictors. However, feature extraction methods are the techniques employed for the selection of the dominant predictors for downscaling modeling with maximum impact. Cheng *et al.* (2005) applied feature extraction methods for hydro-climatic variables' modeling using fuzzy model and coupled genetic algorithm. Pahlavan *et al.* (2017) employed feature extraction method via mutual information (MI) for predictors screening for downscaling modeling using SDSM. Okkan (2015) applied data preprocessing methods of MI and correlation coefficient (CC) for variables' input selection. Despite an increase in variation threats caused by climate change on hydro-climatological variables, previous studies show no efforts have been made to ascertain and evaluate the impact that the climate change may have on precipitation and temperature in North Cyprus through statistical downscaling. Therefore, to fill this gap, this study employed the applications of AI-based (ANN and ANFIS) and MLR statistical downscaling techniques for precipitation and temperature projections over Famagusta (Mağusa), Nicosia (Lefkoşa), and Kyrenia (Girne) stations. Among the several methods of data preprocessing for feature extraction of dominant predictors, MI and CC were found to be exceptional, with remarkable performance and, therefore, were used in this study for the selection of dominant predictors.

2. MATERIALS AND METHODS

2.1. Famagusta (Mağusa) station

Famagusta is a coastal city, located at a latitude 35.12°N, longitude 33.94°E, and altitude 25 m. The climate of Famagusta is warm and temperate with around 19.3 °C average temperature and around 407 mm average rainfall annually.

2.2. Nicosia (Lefkoşa) station

Nicosia is the capital city of both South and North Cyprus. Nicosia is characterized by hot summers and wet winters and, as such, daytime maximum temperature and night-time minimum temperature difference is greater than in the coastal cities. Comparing the other coastline cities' daytime temperature with Nicosia, there is a difference of up to 4 °C or 7 °C for the hottest months of July and August. In the coldest months of January and February, up to 2 °C or 3 °C lower daytime temperature difference is witnessed in Nicosia than other coastal cities.

2.3. Kyrenia (Girne) station

Kyrenia is a coastal city in North Cyprus. The city is situated at a latitude of 35.34°N, longitude of 33.32°E, and altitude of 3 m. The average temperature in the hottest month of July is 29 °C and in the coldest month of January 10 °C. Rainfall in hilly areas varies from 750 mm to as low as 500 mm, falls mostly in winter and on rare occasions in summer. Due to elevation, the highest rainfall is experienced in the Kyrenia Mountains at a rate which ranges between 750 and 1,110 mm. Figure 1 shows a map of Cyprus and locations of the study and the selected grid point.

**Figure 1** | Study locations and the selected grid point.

2.4. Study data

The mean monthly predictands data of precipitation and temperature used in this study from 1995 to 2017 (23 years) were obtained from North Cyprus Meteorological Organization. A total of 13 GCM predictors for a grid point located at Karfas for BNU-ESM GCM under Representation Concentration Pathways (RCPs) from CMIP5 was downloaded from http://cera-www.dkrz.de for large-scale predictors from 1995 to 2040 for the statistical downscaling and future projection of the predictands. Table 1 and Figure 2 give the descriptive statistics of the predictands and precipitation time series from 1995 to 2017 for all stations.

From the displayed precipitation time series in Figure 2 it can be deduced that the precipitation patterns for Famagusta, Nicosia, and Kyrenia are similar, which might be due to their identical semi-arid climate. Despite this development, a difference in the amount or rate of precipitation can be seen from the highest precipitation station (Kyrenia) to the lowest precipitation station (Famagusta). This is in agreement with the characteristics of the data shown in Table 1. In spite of the coastal location of Famagusta station, which by virtue of the larger evaporation body (e.g., sea) would experience higher precipitation than the inland (Nicosia) station, the time series data plotted in Figure 2 show more precipitation was received by Nicosia than Famagusta. This might be because both Nicosia and Kyrenia are surrounded by mountains and the energy reaching the Earth's surface which helps in evaporation and eventual precipitation will reach the mountains faster and, as such, may aggravate precipitation which may lead to receiving more rainfall in mountainous areas. Moreover, from the water cycle concept, water is in constant movement from the Earth to the atmosphere and due to such movement, the water that evaporates from a given area may fall in another area. This implies that a large quantity of water that evaporates from Famagusta may not fall in Famagusta, rather, a small quantity of water that evaporates from another area may fall in Famagusta due to the continuous movement of the water in the atmosphere. Figure 3 gives the temperature time series from 1995 to 2017 for all stations.

Table 1 | Data description for predictands

Station	Parameters	Unit	Min.	Max.	Average	St. deviation
Famagusta (Mağusa)	Precipitation (P_R)	mm	0	5.33	0.77	0.93
	Mean temperature (T_{mean})	°C	12.37	31.23	21.47	5.88
Kyrenia (Girne)	Precipitation (P_R)	mm	0	189.69	27.69	33.13
	Mean temperature (T_{mean})	°C	11.16	30.96	20.61	6.11
Nicosia (Lefkosa)	Precipitation (P_R)	mm	0	5.83	0.94	1.11
	Mean temperature (T_{mean})	°C	10.76	33.26	24.17	6.85
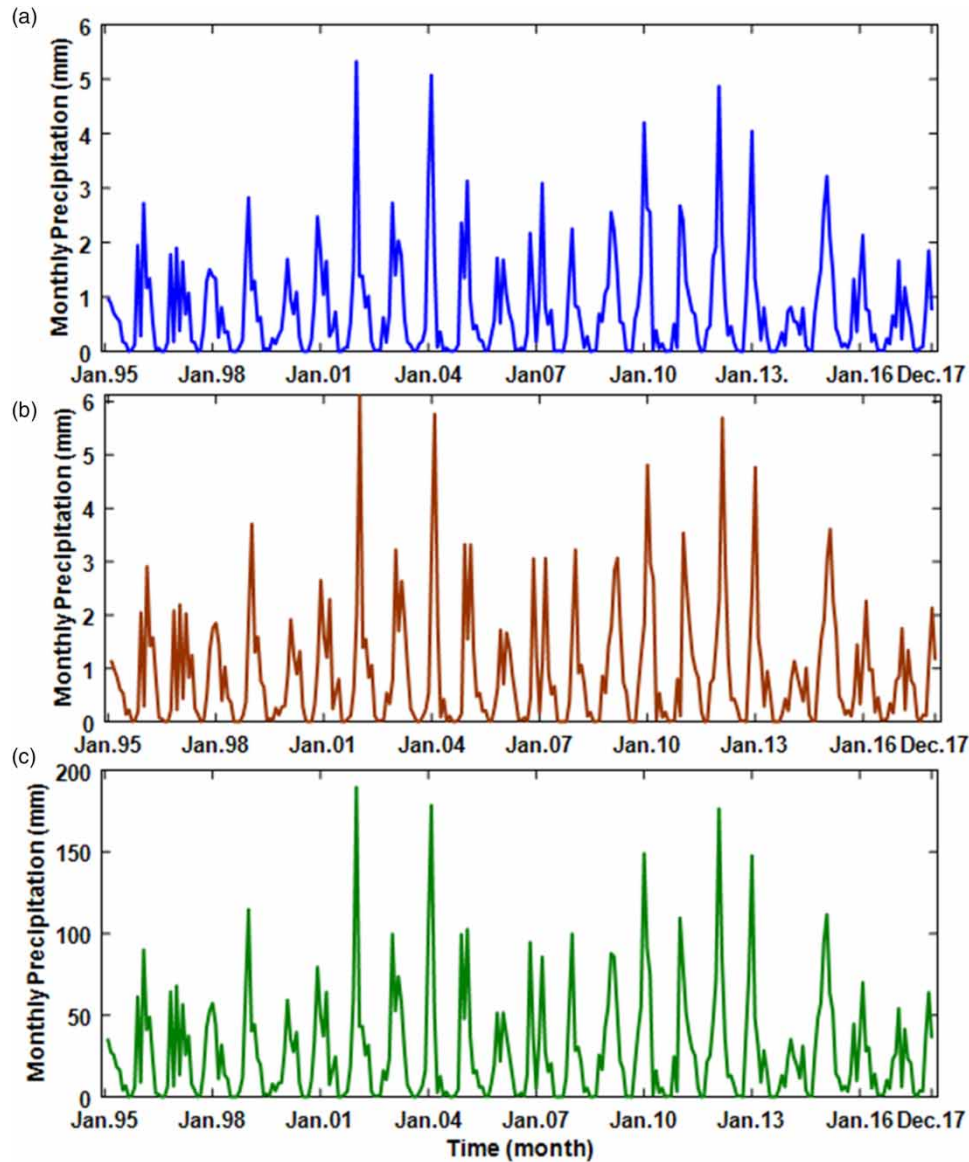
Figure 2 | Precipitation time series from 1995 to 2017 for (a) Famagusta station, (b) Nicosia station, and (c) Kyrenia station.

Table 2 describes the GCM data employed for the study.

As seen in Table 2, the predictors used for the purpose of the study include variables that are related to the factors influencing both precipitation and temperature such as wind speed, relative humidity, temperature, precipitation, etc. at surface and near surface heights.

2.4.1. Data normalization and performance criteria

The data in this study were normalized as follows:

$$P_n = \frac{P_i - P_{min}}{P_{max} - P_{min}} \tag{1}$$

where P_n, P_i, P_{max} and P_{min} are the normalized value, ith observed value, maximum value, and minimum value, respectively.
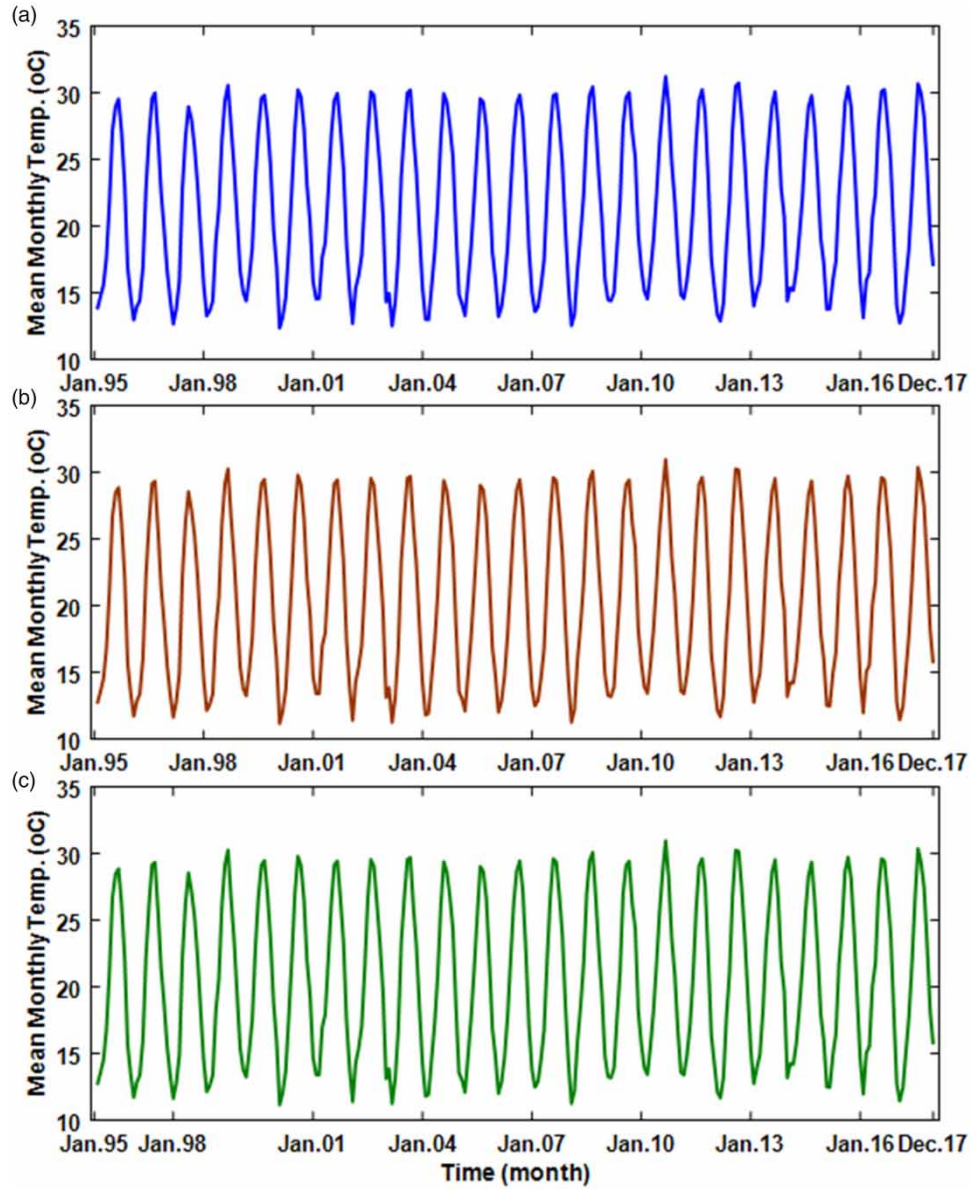
Figure 3 | Temperature time series from 1995 to 2017 for (a) Famagusta station, (b) Nicosia station, and (c) Kyrenia station.

To determine the models' performance, determination coefficient (DC) and root mean square error (RMSE) were employed (Legates & McCabe 1999), given by:

$$DC = 1 - \frac{\sum\limits_{i=1}^{N} (P_i - \hat{P}_i)^2}{\sum\limits_{i=1}^{N} (P_i - \bar{P})^2} \tag{2}$$

$$RMSE = \sqrt{\frac{\sum\limits_{i=1}^{N} (P_i - \hat{P}_i)^2}{N}} \tag{3}$$

where P_i is the observed i^th value, $\bar{P}$ represents mean of the observed values, $\hat{P}_i$ is the predicted i^th value, and N stands for number of observations. The DC has values which range between −infinity and 1 ($-\infty < DC \leq 1$) and the model is more

Table 2 | Data descriptions of large-scale GCM predictors

S/N	Predictors	Description	Height
1	Tasmax	Maximum air temperature	Surface
2	Ts	Sea surface temperature	Surface
3	Hurs	Relative humidity	Near surface
4	Huss	Specific humidity	Near surface
5	Psl	Sea level pressure	Surface
6	Evspsbl	Water evaporation	Surface
7	Sfcwind	Wind speed	Near surface
8	Ps	Surface air pressure	Surface
9	Uas	Zonal wind speed	Near surface
10	Vas	Meridional wind speed	Near surface
11	Prw	Atmospheric water vapor content	Surface
12	Pr	Precipitation	Surface
13	Clwvi	Cloud condensed water content	Surface

efficient with a value close to 1 while RMSE lies between 0 and infinity ($0 \geq \text{RMSE} < \infty$) with the efficiency of the model increasing with RMSE towards 0 (Nourani *et al.* 2020).

2.5. Model validation

In this thesis, k-fold random division of the data set was done for $k = 4$ (four-fold) subsamples. In this way, three-quarters of the subsample were utilized for training and the one-quarter remaining subsample utilized for model validation. The process was repeated four consecutive times, with different three-quarter and one-quarter subsamples for training and validation.

2.6. Proposed methodology

The proposed methodology is in three steps as follows.

2.6.1. Step 1: feature extraction of dominant predictors

For different GCMs, there are different methods of obtaining outputs due to different resolutions; as a result, the reliability of the different GCMs determines the projection efficiency for the future. Therefore, GCM performance assessment and determination of the most dominant GCMs become important (Nourani *et al.* 2019a, 2019b). In this way, CC and MI feature extraction methods were used to calculate predictands (precipitation and temperature) and predictors (GCM outputs) relationships in the form of linear and nonlinear approaches, which led to the selection of dominant predictors used as inputs for the downscaling modeling.

2.6.2. Step 2: statistical downscaling modeling of precipitation and temperature

The statistical downscaling of precipitation and temperature using ANN and ANFIS models was performed in this step considering the dominant predictors determined by feature extraction methods in step 1.

In accordance with the technical literature survey that was conducted, it was found that the evaluation of the AI-based models' downscaling efficiency has been carried out mostly using classic models such as SDSM. In statistical downscaling modeling, SDSM is a commonly applied method which determines predictant and predictors statistical relevance through utilization of MLR method. Hence, MLR model was also employed for the statistical downscaling of the predictands to compare and evaluate the performance of AI-based (ANN and ANFIS) downscaling models. The reason why MLR was preferred over SDSM downscaling model is that, in any time scale, MLR can use predictors, whereas predictors can only be used in daily scale using the SDSM model. In view of this study's monthly time scale, working with the model that uses only daily time scale is not possible. In the next step (step 3), the downscaling model that produced the highest efficiency was used as a benchmark for the projection of future precipitation and temperature.

### 2.6.3. Step 3: future projection of precipitation and temperature

The future projection of monthly precipitation sum and mean temperature for the future from 2018 to 2040 was conducted using the best downscaled model as benchmark output. It is important to mention that due to social, population, energy extension and economic growth rate, future anthropogenic functions are admissibly plausible, which have an impact on greenhouse gas production. According to the future projection above, RCPs represent emission scenario and radiative forcing pathways and were used for precipitation and temperature in the future projection. Detailed information regarding RCPs and emission scenarios can be found in Nourani *et al.* (2019a, 2019b) study. Figure 4 shows the schematic procedure developed for the proposed modeling. It should be noted that the proposed methodology is the same for both precipitation and temperature and is applied for all stations.

2.7. Artificial neural network (ANN)

Among AI techniques, ANN is a convincing approach that has the potential to handle noisy, nonlinearity, and data dynamism, more specifically when there is insufficient understanding of the underlying physical relationships. This emphasizes the ANN as an important data-driven tool for time series modeling (Abdullahi & Elkiran 2017; Nourani *et al.* 2020).

ANN comprises neurons or nodes interconnected by a number of simple processing elements with processing characteristics of attractive peculiarity of information including generalization capability, nonlinearity, learning, parallelism, and noise tolerance. For handling many problems in engineering, a feed forward neural network (FFNN) model equipped with an algorithm called back propagation (BP), among neural network methods, is mostly used (Hornik *et al.* 1989). The method of FFNN constitutes layers of neurons of parallel processing elements, whereby weights are used to connect fully every layer to the proceeding layer. The BP algorithm is generally used to accomplish such ANNs' learning (Hornik *et al.* 1989).

Levenberg–Marquardt (LM), among several algorithms for neural networks' training, was preferred in this study owing to its ability to converge quickly (Sahoo *et al.* 2005). As a hybrid technique and for optimal convergence of solution, the LM algorithm utilizes Gauss–Newton and steepest descent together. The hybrid approach to solve problems of wide margins, usually, different algorithms' best characteristics are used for trade off. For example, the approach of Gauss–Newton is quicker when the optimal solution is relatively close to the initial guess, consequently, the LM algorithm is utilized. Contrarily, the approach of steepest descent is used by the LM algorithm to find an area of potential solution and traverse the design space and then determine the optimum. This technique is especially important for providing solutions to nonlinear equations (Wilson & Mantooth 2013). Nevertheless, the tangent sigmoid (tansig) was utilized as the transfer function of both layers
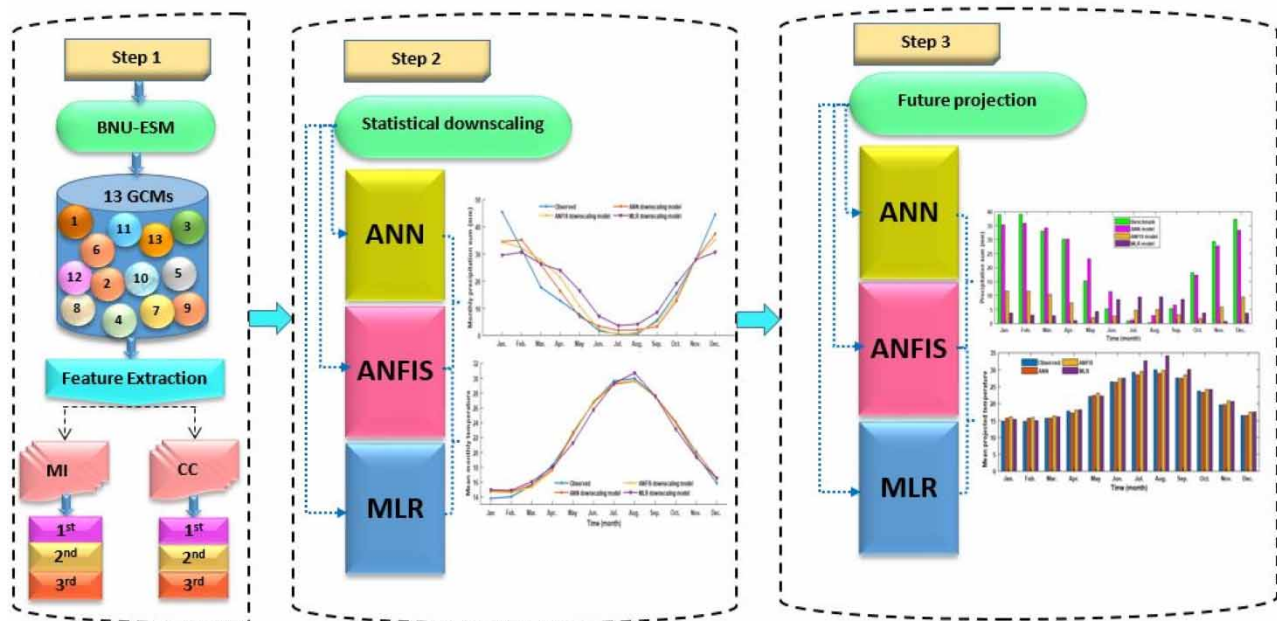
Figure 4 | The applied study methodology.

(hidden and output). To ensure hidden layer neurons of optimum number and also to generate efficient epochs for calibration, a process of trial and error was followed.

2.8. Adaptive neuro fuzzy inference system (ANFIS)

'Neuro fuzzy' in neural network technical literature refers to the approaches of fuzzy logic modeling that comprise distinctive learning algorithm application to the system of fuzzy inference (FIS). In the development of neuro fuzzy system, ANFIS is a peculiar approach that Jang (1993) initially introduced. It utilizes the learning algorithm of the neural network.

Every fuzzy system is constituted of three major parts, namely: fuzzifier, defuzzifier, and fuzzy database (Nourani *et al.* 2015). Inference engine and fuzzy rule base are fuzzy database's two essential parts. Rules related to fuzzy propositions are contained in fuzzy rule base as Jang *et al.* (1997) revealed. Therefore, in fuzzy inference, operational analysis is administered. The fuzzy inference engines that are most commonly applied are Mamdani and Sugeno, both of which could produce a desired goal on application.

For overall real continuous functions, ANFIS being a universal approximator is capable of impacting accuracy to a higher degree. As Jang *et al.* (1997) stated, functionally, ANFIS is equivalent to FIS. Thus, specifically, the ANFIS system is equal to first order Sugeno fuzzy model. Figure 4 shows ANFIS general structure. As seen in Figure 4, the ANFIS model has x and y inputs with f considered as output. There are two if-then sets of rules constituted in the first order Sugeno model, demonstrated as:

$$\text{Rule (1): If } \mu(x) \text{ is } A_1 \text{ and } \mu(y) \text{ is } B_1; \text{ the } f_1 = p_1 x + q_1 y + r_1 \tag{4}$$

$$\text{Rule (2): If } \mu(x) \text{ is } A_2 \text{ and } \mu(y) \text{ is } B_2; \text{ the } f_2 = p_2 x + q_2 y + r_2 \tag{5}$$

where x inputs' membership functions (MFs) are represented by A_1 and A_2, while y inputs' MFs are represented by B_1 and B_2. p_1, q_1, r_1 and p_2, q_2, r_2 are output function parameters.

Each ANFIS layer has the following functions:

Layer 1: Input variable membership grades are produced by each node in this layer. The ith node output of the k layer is denoted by Q_i^k. Assuming as a generalized bell function of a MF (gbellmf), Jang & Sun (1995) stated that the output (Q_i^1), can be determined from:

$$Q_i^1 = \mu_{A_i}(x) = \frac{1}{1 + ((x - c_i)/a_i))^{2b_i}} \tag{6}$$

where a_i, b_i, c_i are adaptable variables called premise parameters.

Layer 2: In this layer, the incoming signals are multiplied by each node:

$$Q_i^2 = w_i = \mu_{A_i}(x). \mu_{B_i}(y) \; i = 1, \; 2, \; \ldots \tag{7}$$

Layer 3: In this layer, the ith node calculated the normalized firing strength:

$$Q_i^3 = \bar{w}_i = \frac{w_i}{w_1 + w_2} i = 1, \; 2 \tag{8}$$

Layer 4: In this layer, node i calculated the contribution given by the ith rule to the model output:

$$Q_i^4 = \bar{w}_i(p_i x + p_i y + r_i) = \bar{w}_i f_i \tag{9}$$

where p_1, q_1, r_1 is the perimeter set, $\bar{w}_i$ is the output of layer 3.

Layer 5: In this layer, a single node calculated the overall output of the ANFIS (Jang & Sun 1995):

$$Q_i^5 = \sum_i \bar{w}_i f_i = \frac{\sum_i w_i f_i}{\sum_i w_i} \tag{10}$$

ANFIS hybrid learning algorithm is formed by a combination of least-squares and gradient descent methods. The consequent parameters are represented by p_i, q_i, r_i while the optimization parameters known as premise parameters are represented by a_i, b_i, c_i. Least-square technique identified the consequent parameter in the hybrid learning approach towards forward pass until the fourth layer where the output node goes forward. There is propagation of the error signals backward in the backward pass and the gradient descent updated the premise parameters (Nourani & Komasi 2013).

2.9. Multiple linear regression (MLR)

MLR is a conventional technique that models mathematically the linear relevancy between two or more predictors (independent variables) and a predictand (dependent variable). In general, the n and y representing predictors and dependent variables might have a relation, given by (Nourani *et al.* 2019a, 2019b):

$$y = b_0 + b_1 x_1 + b_2 x_2 + b_3 x_3 + \ldots + b_i x_i + \xi \tag{11}$$

where the *i*th predictor value is x_i, the constant of regression is b_0, the *i*th predictor coefficient is b_i and the error term is ξ. Figure 4 shows a visual MLR model.

2.10. Correlation coefficient (CC)

The method of CC has been applied as a common metric for understanding the linear behavior between variables (predictand and predictors). Its values fall between $+1$ and -1 (Baghanam *et al.* 2019).

2.11. Mutual information (MI)

Using data probability distribution, mathematically the information and entropy content have been measured and formulated (Shannon 1948).

2.12. Model validation

In this thesis, k-fold cross-validation technique was utilized to validate the models. With k-fold technique, the data set is divided randomly into a certain number of equal subsamples regarded as k-number subsamples. The model is trained with the k-number subsamples minus 1 (k − 1) and the remaining k-subsample is used for validation. The process is repeated continuously with k − 1 and k different subsamples for training and validation of the model, until the subsamples are used once in both training and validation of the model. The final results are then obtained by averaging the k-fold results. The advantage of k-fold validation technique is that for model training and validation, every observation is used once (Nourani *et al.* 2019a, 2019b).

In this study, the k-fold random division of the data set was done for k = 4 (four-fold) subsamples. In this way, three-quarters of the subsample were utilized for training and the one-quarter remaining subsample utilized for model validation. The process was repeated four consecutive times, with different three-quarter and one-quarter subsamples for training and validation.

3. RESULTS AND DISCUSSION

This study was performed in three steps. In the first step, the most appropriate downscaling predictors were determined using the methods of MI and CC in order to have better downscaling modeling of precipitation and temperature. Statistical downscaling modeling was performed in the second step through the application of ANN and ANFIS nonlinear downscaling models and compared with linear MLR downscaling model. In the final step (step 3) of this study, future projection of precipitation and temperature was conducted. Therefore, the results in this study were presented accordingly.

3.1. Step 1 results (selection of downscaling predictors for predictands)

The results of the applied MI feature extraction technique are presented in Tables 3 and 4. It should be understood that a predictor with higher MI signifies the dominant predictor for the predictand.

As depicted by the MI results in Table 3, different predictors characterize different performance for certain predictands for different stations. For Famagusta station, the results show that Huss (1.6735), Uas (1.6698), and Sfcwind (1.6633) are, respectively, ranked as the first, second, and third most dominant predictors with respect to precipitation predictand. These are relative humidity and wind speed related predictors. According to the results provided by Allen *et al.* (1998) study, relative humidity and wind speed are important parameters in the hydrologic water cycle whereas precipitation is among the most significant parameters. This shows that the relationship and bonding (between precipitation, relative humidity, and wind speed) are not affected by local-scale climate but they are strong for large-scale climate. For temperature, the most dominant predictors are Clwvi (1.6035), Huss (1.5972), and Uas. This shows that both Huss and Uas have a strong nonlinear

Table 3 | Step 1 results across the study stations for MI input screening

Station	Predictor	Precipitation		Temperature	
		MI	Rank	MI	Rank
Famagusta	Tasmax	1.6374	6	1.5568	6
	Ts	1.6293	8	1.5403	8
	Hurs	1.6460	5	1.5687	5
	Huss	1.6735	1	1.5972	2
	Psl	1.6604	4	1.5480	7
	Evspsbl	1.6069	9	1.5253	10
	Sfcwind	1.6633	3	1.5850	4
	Ps	1.6297	7	1.5272	9
	Uas	1.6698	2	1.5968	3
	Vas	1.6015	10	1.5188	11
	Prw	1.4028	12	1.3135	13
	Pr	1.5086	11	1.4112	12
	Clwvi	1.3674	13	1.6035	1
Nicosia	Tasmax	1.6335	6	1.5868	7
	Ts	1.6261	7	1.5645	8
	Hurs	1.6783	3	1.6059	6
	Huss	1.7020	1	1.6316	1
	Psl	1.6732	5	1.6168	5
	Evspsbl	1.5368	10	1.4711	11
	Sfcwind	1.6776	4	1.6213	3
	Ps	1.6071	8	1.5476	9
	Uas	1.6951	2	1.6189	4
	Vas	1.5866	9	1.5342	10
	Prw	1.3786	13	1.3169	13
	Pr	1.4906	11	1.4218	12
	Clwvi	1.3891	12	1.6311	2
Kyrenia	Tasmax	1.6902	9	1.6161	9
	Ts	1.7483	4	1.6622	2
	Hurs	1.7367	7	1.6362	7
	Huss	1.7468	5	1.6484	6
	Psl	1.7621	3	1.6567	3
	Evspsbl	1.7393	6	1.6289	8
	Sfcwind	1.7707	2	1.6492	5
	Ps	1.7149	8	1.6031	10
	Uas	1.7727	1	1.6648	1
	Vas	1.6661	10	1.5503	11
	Prw	1.4755	12	1.3610	13
	Pr	1.5585	11	1.4506	12
	Clwvi	1.4386	13	1.6566	4

Table 4 | Step 1 results across the study stations for CC input screening

Station	Predictor	Precipitation		Temperature	
		CC	Rank	CC	Rank
Famagusta	Tasmax	−0.6220	13	0.9686	1
	Ts	−0.4911	10	0.9379	3
	Hurs	−0.2787	7	0.1731	7
	Huss	−0.5641	12	0.9459	2
	Psl	0.6356	1	−0.8804	13
	Evspsbl	0.5168	5	−0.4202	8
	Sfcwind	−0.3216	8	0.5200	5
	Ps	0.5473	4	−0.6790	9
	Uas	−0.3523	9	0.2119	6
	Vas	0.5482	3	−0.8714	12
	Prw	−0.5378	11	0.8505	4
	Pr	0.5162	6	−0.7246	10
	Clwvi	0.5781	2	−0.7493	11
Nicosia	Tasmax	−0.6230	13	0.9677	1
	Ts	−0.4956	11	0.9304	3
	Hurs	−0.3636	9	0.5010	5
	Huss	−0.5689	12	0.9611	2
	Psl	0.5832	1	−0.7114	11
	Evspsbl	0.2197	6	0.0349	7
	Sfcwind	−0.0862	7	0.0042	8
	Ps	0.5168	4	−0.6915	9
	Uas	−0.1020	8	0.0838	6
	Vas	0.5563	3	−0.8640	13
	Prw	−0.4651	10	0.8102	4
	Pr	0.4995	5	−0.7094	10
	Clwvi	0.5750	2	−0.7584	12
Kyrenia	Tasmax	−0.6184	13	0.9732	1
	Ts	−0.5153	11	0.9400	3
	Hurs	0.6448	1	−0.8769	13
	Huss	−0.5814	12	0.9551	2
	Psl	0.6209	3	−0.7112	8
	Evspsbl	0.1475	7	0.0296	7
	Sfcwind	−0.0963	8	0.0871	5
	Ps	0.6233	2	−0.8763	12
	Uas	−0.2456	9	0.0501	6
	Vas	0.5004	6	−0.8757	11
	Prw	−0.4651	10	0.7664	4
	Pr	0.5295	5	−0.7217	9
	Clwvi	0.6184	4	−0.7636	10

relationship with the predictands (precipitation and temperature). This may be because Famagusta is a semi-arid coastal station which is both affected by the characteristics of hot temperature and insufficiency of rainfall.

Despite the nonlinearity effect displayed by predictors, it is a well-known fact that time series data may contain both linear and nonlinear aspects not only for local-scale data but also for large-scale data. Therefore, in order to determine the linear relationship between the predictors and the predictands, the CC method of input screening was performed. The results of the applied CC method of feature extraction are presented in Table 4.

In the results shown in Table 4, it can be seen that some variables have a negative relationship with the predictands while some have positive values. For Famagusta station, considering precipitation as the predictand, the pressure-related predictor (Psl) was found to be most effective followed by wind speed-related predictors (Clwvi and Vas). By comparing with the results achieved by the MI method, in Famagusta station, it is obvious that due to the linear and nonlinear nature of the feature extraction methods, distinct results were obtained. For example, Clwvi is found to be the least effective predictor variable

using the MI method, while the CC method showed Clwvi as the most dominant predictor. However, as shown in Table 4, Tasmax, Huss, and Ts are, respectively, the best, second, and third most sensitive predictors with temperature as the predictand. This demonstrates that the linear correlation is stronger towards temperature variable. With the determination of the significant predictors, the statistical downscaling modeling was then performed and the results are presented in the next section.

3.2. Step 2 results (statistical downscaling modeling)

The network parameters used to develop the ANN model including learning algorithm, transfer function type, training function, etc. for the two predictands under study for all stations are presented in Table 5.

For ANFIS downscaling modeling, hybrid optimization algorithm was used for the calibration of Sugeno type fuzzy inference system. Several membership functions were used including Trapezoidal, Triangular and Gaussian. To achieve the best ANFIS construction, trial and error procedure was employed for the network selection. The parameters used in developing ANFIS downscaling modeling are presented in Table 6.

It is important to state that since the study is concerned with statistical downscaling modeling of precipitation and temperature, the results are presented in different subsections for all stations.

3.2.1. Statistical downscaling of precipitation

The results of the downscaling modeling of precipitation using the ANN, ANFIS, and MLR downscaling models for both MI and CC predictor screening methods across the study stations are provided in Table 7. It is worth clarifying that the results are presented for the best downscaling performance.

Table 5 | ANN network parameters for statistical downscaling modeling

Station	Model function	Precipitation		Temperature	
		MI	CC	MI	CC
Famagusta	Type of network used	FFNN	FFNN	FFNN	FFNN
	Learning algorithm	LM	LM	LM	LM
	Training function	TrainLM	TrainLM	TrainLM	TrainLM
	Number of input layer neurons	3	3	3	3
	Number of hidden layer neurons	8	6	12	10
	Number of output layer neurons	1	1	1	1
	Transfer function type	TANSIG	TANSIG	TANSIG	TANSIG
	Maximum epochs	1,000	1,000	1,000	1,000
	Number of iterations	236	198	70	150
Nicosia	Type of network used	FFNN	FFNN	FFNN	FFNN
	Learning algorithm	LM	LM	LM	LM
	Training function	TrainLM	TrainLM	TrainLM	TrainLM
	Number of input layer neurons	3	3	3	3
	Number of hidden layer neurons	7	7	7	7
	Number of output layer neurons	1	1	1	1
	Transfer function type	TANSIG	TANSIG	TANSIG	TANSIG
	Maximum epochs	1,000	1,000	1,000	1,000
	Number of iterations	300	276	300	276
Kyrenia	Type of network used	FFNN	FFNN	FFNN	FFNN
	Learning algorithm	LM	LM	LM	LM
	Training function	TrainLM	TrainLM	TrainLM	TrainLM
	Number of input layer neurons	3	3	3	3
	Number of hidden layer neurons	10	7	6	6
	Number of output layer neurons	1	1	1	1
	Transfer function type	TANSIG	TANSIG	TANSIG	TANSIG
	Maximum epochs	1,000	1,000	1,000	1,000
	Number of iterations	120	96	120	96

FFNN, LM, and TANSIG represent feed forward neural network, Levenberg–Marquardt, and tangent sigmoid, respectively.

Table 6 | ANFIS network parameters for statistical downscaling modeling

Station	Model function	Precipitation		Temperature	
		MI	CC	MI	CC
Famagusta	Learning algorithm	Hybrid	Hybrid	Hybrid	Hybrid
	Fuzzy inference algorithm	Sugeno	Sugeno	Sugeno	Sugeno
	Structure formulation	TA	TA	TA	TA
	Membership function type	Triangular	Trapezoidal	Gaussian	Triangular
	Generated FIS	GP	GP	GP	GP
	Number of membership functions	3	3	3	3
	Output type	Constant	Constant	Constant	Constant
	Error tolerance	0.0005	0.0005	0.0005	0.0005
	Epochs	53	29	60	77
Nicosia	Learning algorithm	Hybrid	Hybrid	Hybrid	Hybrid
	Fuzzy inference algorithm	Sugeno	Sugeno	Sugeno	Sugeno
	Structure formulation	TA	TA	TA	TA
	Membership function type	Trapezoidal	Trapezoidal	Gaussian	Gaussian
	Generated FIS	GP	GP	GP	GP
	Number of membership functions	3	3	3	3
	Output type	Constant	Constant	Constant	Constant
	Error tolerance	0.0001	0.0001	0.0001	0.0003
	Epochs	70	102	39	82
Kyrenia	Learning algorithm	Hybrid	Hybrid	Hybrid	Hybrid
	Fuzzy inference algorithm	Sugeno	Sugeno	Sugeno	Sugeno
	Structure formulation	TA	TA	TA	TA
	Membership function type	Triangular	Gaussian	Gaussian	Trapezoidal
	Generated FIS	GP	GP	GP	GP
	Number of membership functions	3	3	3	3
	Output type	Constant	Constant	Constant	Constant
	Error tolerance	0.0005	0.0005	0.0005	0.0005
	Epochs	88	110	90	68

GP and TA represent grid partitioning and trial and error.

Table 7 | Statistical downscaling results for precipitation

Station	Input screening method	Downscaling model	Inputs	Training		Validation	
				DC	[a]RMSE	DC	[a]RMSE
Famagusta	MI	ANN	Huss, Uas, Sfcwind	0.589	0.097	0.554	0.121
		ANFIS	Huss, Uas, Sfcwind	0.546	0.101	0.518	0.126
		MLR	Huss, Uas, Sfcwind	0.404	0.116	0.377	0.143
	CC	ANN	Psl, Clwvi, Vas	0.438	0.136	0.360	0.120
		ANFIS	Psl, Clwvi, Vas	0.507	0.106	0.497	0.129
		MLR	Psl, Clwvi, Vas	0.433	0.137	0.355	0.121
Nicosia	MI	ANN	Huss, Uas, Hurs	0.408	0.116	0.404	0.142
		ANFIS	Huss, Uas, Hurs	0.450	0.127	0.286	0.137
		MLR	Huss, Uas, Hurs	0.337	0.150	0.291	0.126
	CC	ANN	Psl, Clwvi, Vas	0.570	0.121	0.404	0.116
		ANFIS	Psl, Clwvi, Vas	0.563	0.122	0.394	0.117
		MLR	Psl, Clwvi, Vas	0.457	0.136	0.368	0.119
Kyrenia	MI	ANN	Uas, Sfcwind, Psl	0.556	0.099	0.487	0.130
		ANFIS	Uas, Sfcwind, Psl	0.532	0.102	0.581	0.118
		MLR	Uas, Sfcwind, Psl	0.435	0.137	0.413	0.114
	CC	ANN	Hurs, Ps, Psl	0.522	0.126	0.371	0.118
		ANFIS	Hurs, Ps, Psl	0.562	0.120	0.492	0.106
		MLR	Hurs, Ps, Psl	0.475	0.132	0.469	0.108

[a]RMSE: Being normalized data, RMSE is unitless.

As given in Table 7, the downscaling performances of the models are evaluated according to DC and RMSE performance indicators. Considering Famagusta station, it can be seen that the AI downscaling models performed better than MLR downscaling model with respect to both MI and CC predictors' screening methods. In terms of DC and based on validation results, ANN is found to be the more efficient downscaling model with 4 and 17% over ANFIS and MLR, respectively, based on MI feature extraction. In terms of CC, ANFIS outperformed the other models with 14 and 15% over ANN and MLR, respectively.

For Nicosia station, the general performance of the downscaling models is lower in comparison to Famagusta station, especially that obtained by MI method. This could be because of the difference in location of the two stations (inland for Nicosia and coastal for Famagusta). The better performance of models produced by the CC method could be due to the direct effect the environment has on precipitation aspect, in the sense that the energy reaching the area causes a direct increase in temperature and is easily predictable with less fluctuations which result in an almost constant amount of evaporation and transpiration and hence precipitation.

For Kyrenia station, it is expected that the performance of the statistical downscaling models would be higher than in Famagusta and Nicosia stations. This is as a result of a higher amount and frequency of precipitation experienced in Kyrenia station. As the results in Table 7 show, a high amount of precipitation received in an area signifies better downscaling capabilities and, of course, better performance and vice versa. Similar to the coastal station (Famagusta), ANFIS is found to be more efficient than the rest of the downscaling models. To evaluate the monthly precipitation downscaling performance of the applied models, the observed monthly precipitation sum is compared with the downscaled precipitation sum by the applied downscaling models and presented in Figure 5.

It can be seen from Figure 5 that December and January are the months with the highest precipitation amount and the months span from June to August are periods with little or no rainfall amounts across all the study stations. In view of the closeness and fitness of the downscaled models towards the observed precipitation between June and August it can be deduced that the downscaling models are more reliable within that period.

3.2.2. Statistical downscaling of mean temperature

Similarly to precipitation, the results of the downscaling modeling of temperature using the ANN, ANFIS, and MLR downscaling models for both MI and CC predictors' screening methods across the study stations are provided in Table 8. However, the results are presented for the best downscaling performance.

By visual inspection of Tables 7 and 8 it can be understood that the general performance of the downscaling models are more superior in temperature downscaling than precipitation downscaling. This may be because of the distinct characteristics of the predictands in the study stations. Having a semi-arid Mediterranean climate, the stations under study are subjected to high temperature and scarce water resources (less or little rainfall). The harsh weather, coupled with uncertainty in factors affecting hydrologic cycle, leads to a greater stochastic nature of precipitation and, hence, difficulty in downscaling. The results in Table 8 show better downscaling capability of AI models than MLR model across all stations.

For Famagusta station in the validation phase based on DC performance indicator, the results in Table 8 revealed that ANFIS produced the best performance in terms of MI. ANFIS improved performance in the mean temperature downscaling modeling up to 1 and 3% over ANN and MLR, respectively. Regarding the CC feature screening method, ANN was the best performing downscaling model with an improvement of 1% over ANFIS and 3% over MLR. For Nicosia station, ANFIS had the best performance with DC 0.959, followed by ANN with 0.944 and, finally, MLR with 0.941 with respect to MI, whereas ANN slightly edged out ANFIS with DCs of 0.970 and 0.968, and MLR followed with DC of 0.951. For Kyrenia station, ANFIS was narrowly the best downscaling model with DC of 0.959 and RMSE 0.063, followed by ANN with DC of 0.954 and RMSE 0.066. The MLR downscaling model performed the least with DC of 0.926 and RMSE 0.084. To ascertain the performances of the downscaling models for mean temperature in the period of this study (1995–2017), the monthly average of the statistically downscaled temperature for each month is compared with the observed mean temperature, as shown in Figure 6.

Figure 6 shows the downscaling models are very close to the observed values which ultimately confirmed the performance illustrated by DC and RMSE efficiency criteria. However, when the downscaling results of Figures 5 and 6 are compared, it can be deduced that values in Figure 6 are more fitted to observed values. This indicates that better downscaling modeling is achieved with temperature as predictand than with precipitation. Moreover, Figure 6 indicates that temperature within the study region is higher in hot months (most especially the hottest months of June, July, August, and September) and lower in cold months (December, January, February, and March).
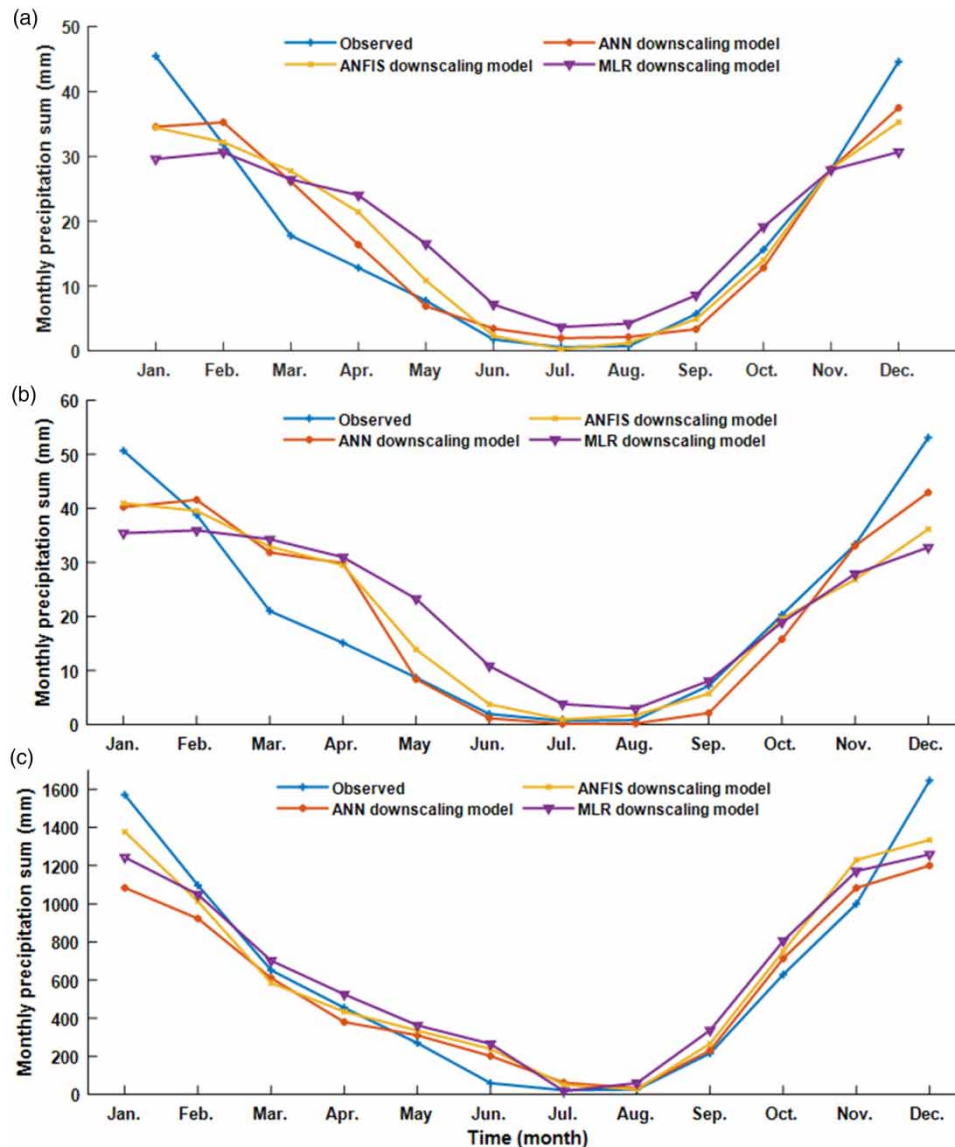
Figure 5 | Comparison of monthly precipitation between observed and downscaling models for (a) Famagusta station, (b) Nicosia station, and (c) Kyrenia station.

3.3. Step 3 results (future projection of precipitation and temperature)

The results for the future projection of precipitation and temperature are provided in two subsections.

3.3.1. Results of precipitation projection for the future

It can be seen from Table 8 that in most cases ANN provided the best performance for the downscaling modeling using MI feature extraction method, while ANFIS mostly performed better for CC method. Therefore, for future projection of precipitation, ANN was used as the benchmark model for projection made based on MI method and ANFIS was used as the benchmark model for projection based on CC method. Figure 7 compares the benchmark monthly precipitation sum and future projection by the applied models.

Since the projection results showed that the ANN model performed better in the projection of precipitation for the future, the discussion in the section is done through comparison between benchmark precipitation and future projection by ANN model only. Considering the projected precipitation sum for Famagusta station it can be seen that, in almost every month, there would be a decrease in the precipitation amount with the exception of May and August. This could be because the

Table 8 | Statistical downscaling results for temperature

| Station	Input screening method	Downscaling model	Inputs	Training DC	Training [a]RMSE	Validation DC	Validation [a]RMSE
Famagusta	MI	ANN	Clwvi, Huss, Uas	0.948	0.069	0.940	0.077
		ANFIS	Clwvi, Huss, Uas	0.951	0.067	0.943	0.075
		MLR	Clwvi, Huss, Uas	0.923	0.085	0.914	0.092
	CC	ANN	Tasmax, Huss, Ts	0.976	0.047	0.976	0.049
		ANFIS	Tasmax, Huss, Ts	0.972	0.052	0.969	0.053
		MLR	Tasmax, Huss, Ts	0.954	0.067	0.951	0.067
Nicosia	MI	ANN	Huss, Clwvi, Sfcwind	0.945	0.071	0.944	0.073
		ANFIS	Huss, Clwvi, Sfcwind	0.965	0.056	0.959	0.063
		MLR	Huss, Clwvi, Sfcwind	0.950	0.067	0.941	0.076
	CC	ANN	Tasmax, Huss, Ts	0.970	0.052	0.970	0.054
		ANFIS	Tasmax, Huss, Ts	0.968	0.054	0.968	0.056
		MLR	Tasmax, Huss, Ts	0.953	0.065	0.951	0.069
Kyrenia	MI	ANN	Uas, Ts, Psl	0.958	0.062	0.954	0.066
		ANFIS	Uas, Ts, Psl	0.962	0.058	0.959	0.063
		MLR	Uas, Ts, Psl	0.927	0.081	0.926	0.084
	CC	ANN	Tasmax, Huss, Ts	0.966	0.058	0.963	0.058
		ANFIS	Tasmax, Huss, Ts	0.970	0.053	0.967	0.055
		MLR	Tasmax, Huss, Ts	0.953	0.067	0.953	0.065

[a]RMSE: Being normalized data, RMSE is unitless.

two months serve as the strategic points for the arrival of summer and the entry to winter. It can be seen that periods with higher precipitation including November, December, January, February, and March will experience a greater decrease in precipitation than months with less frequency and amount of precipitation. For instance, a decrease of about 8% could be noticed in November, 14% in December, 12% in January and February, and 5% in March. The results in Figure 7 show a different pattern of precipitation in Nicosia with respect to Famagusta. The precipitation trend shows an increase in precipitation in the summer period (March, May, June, July, August, September) and decreasing trend in October, November, December, January, and February while April remains the same. However, the precipitation decrease is very low in Nicosia compared to Famagusta. For instance, a decrease of 0.5, 1, 2, 2, and 2% is observed for October, November, December, January, and February whereas an increase in precipitation values of up to 0.5, 4, 4, 0.2, 2, and 1% are witnessed for March, May, June, July, August, and September, respectively. For Kyrenia station, despite having a different amount of precipitation sum compared to Famagusta, it has a similar percentage decrease in precipitation. The only difference is that throughout the period, there is no increasing trend for precipitation in any month and there is a large percentage decreasing every year.

The general results for the future projection of precipitation showed that towards the middle of the 21st century (2018–2040), the amount of precipitation is expected to decrease within the stations under consideration. Kyrenia station is expected to be more impacted with a reduction of up to 42%. This is because the station experiences the highest precipitation in North Cyprus and it is obvious that the higher precipitation received by a region, the more availability of water to be lost by evapotranspiration and, thus, the difference between the inflows and outflows will be larger compared with an area that received less precipitation. This is proven by the results of this study. However, Famagusta station, due to the presence of sea, receives the second highest precipitation and, hence, second highest decrease up to 22% of precipitation towards 2040. On the other hand, Nicosia being an inland station receives less precipitation and, subsequently, less precipitation decrease of 4.8%.

3.3.2. Results of temperature projection for the future

As depicted by Table 8, both AI downscaling models performed efficiently and, at one point in a certain station and certain input screening method, ANN provided the most reliable performance, whereas in another circumstance, ANFIS is most significant. Moreover, their difference in performance is very small, to the extent that any of them could be efficient if selected for the future projection of temperature. In view of this, ANN statistical downscaled values were selected as the benchmark temperature for all stations. The performance of the models for the future projection of temperature in most cases is higher in Nicosia station for both MI and CC input selection methods. This could be because of the slightly higher temperature that
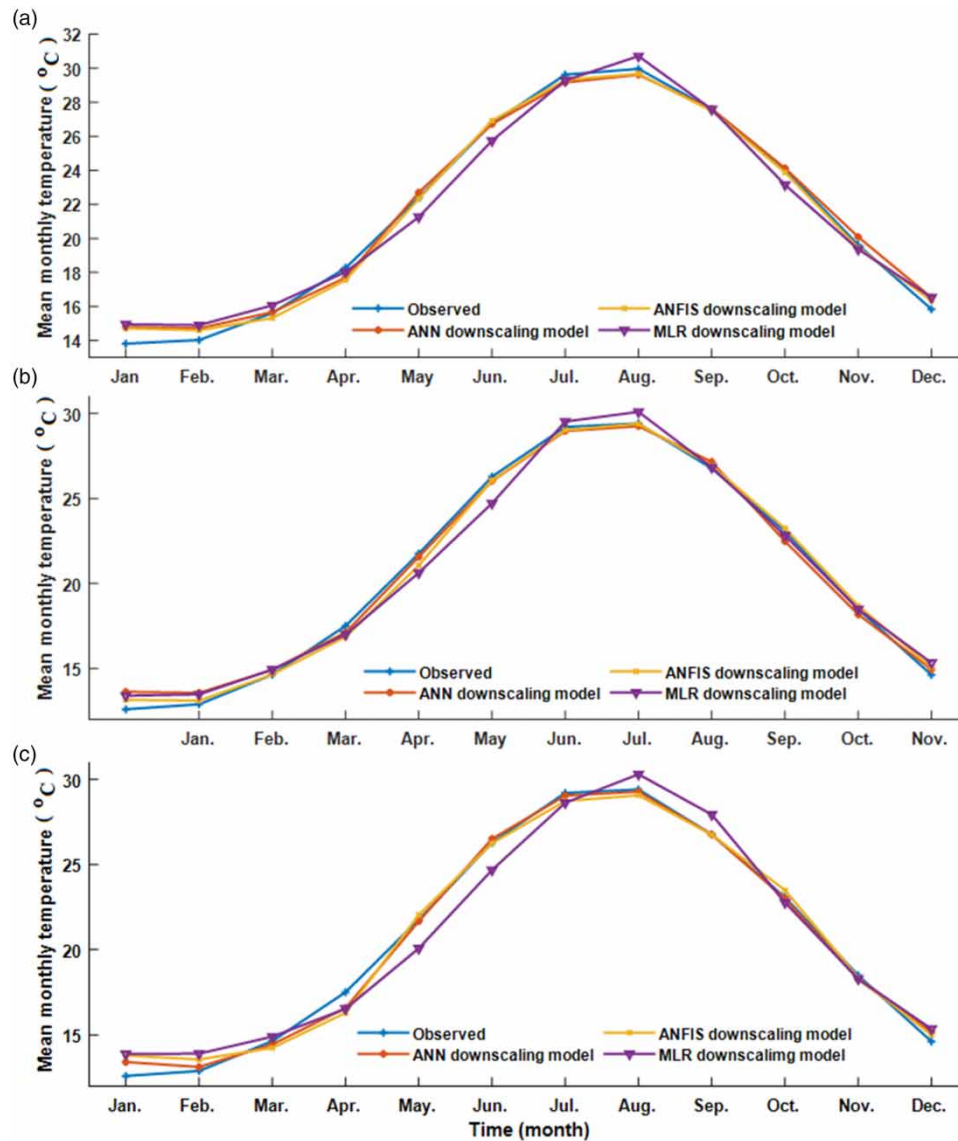
Figure 6 | Comparison of monthly mean temperature between observed and downscaling models for (a) Famagusta station, (b) Nicosia station, and (c) Kyrenia station.

Nicosia is experiencing in comparison to Famagusta and Kyrenia stations (see Table 3). Comparing the performances across the stations, it can be seen that for Famagusta, ANN provided the best performance based on MI, whereas for CC method, ANFIS led to better performance. Since all the three models have shown accuracy in the future projection of temperature, the temperature values produced by the models are compared with the benchmark temperature and presented in Figure 8 to determine the trend of decrease or increase in temperature between 2018 and 2040.

The close temperature trend shown by the models in Figure 8 affirmed the reliable performance of the models indicated by DC and RMSE evaluation criteria in Table 8. However, the future projection of higher mean temperature produced by the MLR model shown in Figure 8 could be due to error produced by the model as can be seen in Table 8. Since ANN and ANFIS models are found to be more robust models as shown in both Table 8 and Figure 8, the discussion regarding the mean temperature for the future is done based on the two models.

For Famagusta station, both ANN and ANFIS models show an increase in the future temperature of less than 1% in the months of January and February. March, May, June, September, November, and December show no difference (decrease or increase) in the mean temperature by ANN model but for the ANFIS model, the months with no difference are April
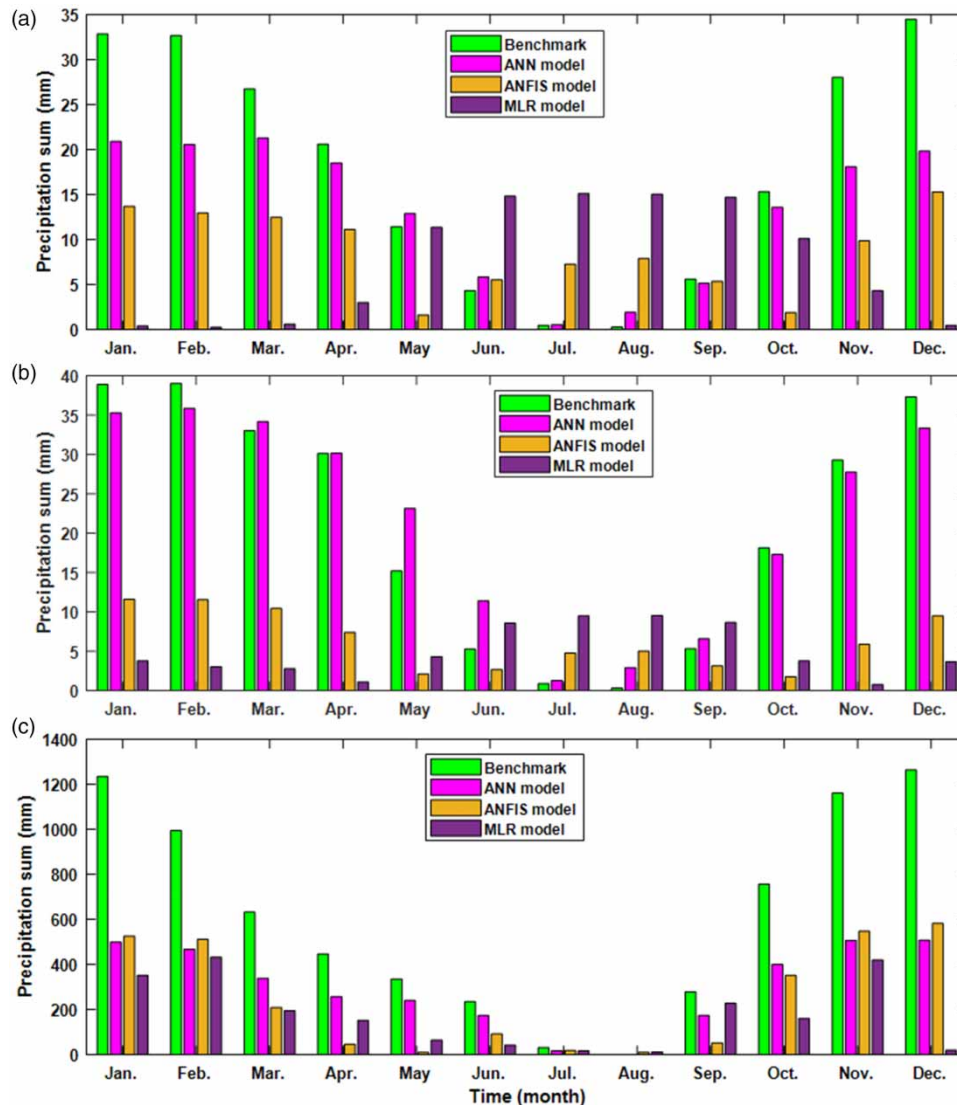
Figure 7 | Monthly projected precipitation sum in the future (2018–2040) for (a) Famagusta station, (b) Nicosia station, and (c) Kyrenia station.

and August only. A decrease in the temperature is noticed in April, July, August, and October. For Nicosia station, an increase in the mean temperature will occur from January through June. This may be because with continuing greenhouse effect, the temperature of hot weather climate increases and gradually even the temperature in cold weather changes. A short decrease of usually less than 1% of mean temperature will occur from July to September while October, November, and December will also witness a rise in temperature. What this implies is that the future temperature for Nicosia will increase in the winter season and slightly increase in summer season. For Kyrenia station, the increase and decrease in the mean temperature is similar to Nicosia station. From November through March the temperature is expected to rise. While April and May show a balance between previous and future mean temperature, June, July, August, September, and October will experience a slight decrease.

The general results of the projected precipitation and mean temperature showed that there will be a decrease in precipitation amount in Kyrenia station in every month of the year from 2018 to 2040, while a decrease in precipitation is also expected for Nicosia and Famagusta stations for all months with the exception of May where the results showed an expected increase in precipitation. With regards to mean temperature, both increase and decrease are possible due to the effect of greenhouse gases. The increase will occur mostly in winter periods while summer periods will experience a decrease in
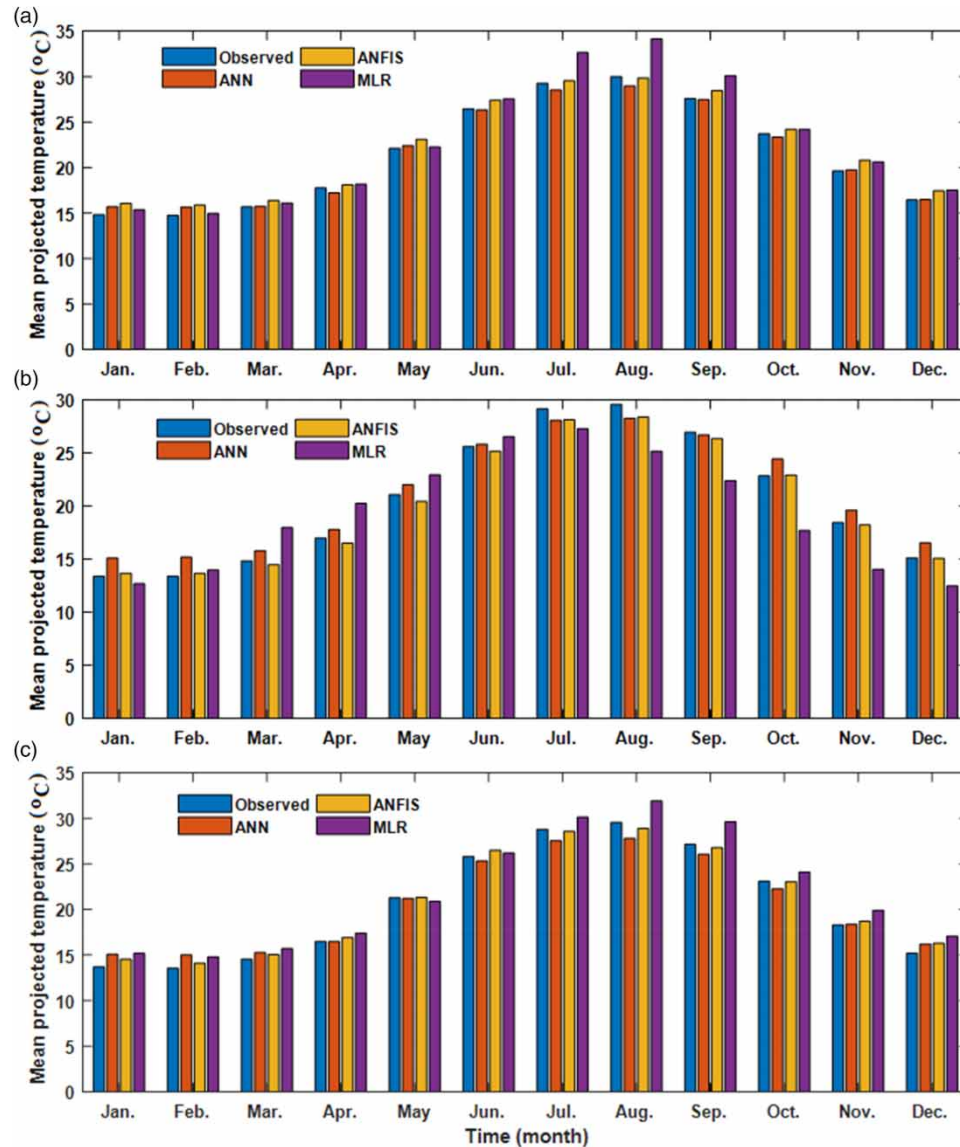
Figure 8 | Monthly projected mean temperature in the future (2018–2040) for (a) Famagusta station, (b) Nicosia station, and (c) Kyrenia station.

temperature. The results also showed that in terms of percentage, a higher percentage of precipitation would be lost compared to an increment or decrease percentage of mean temperature.

4. CONCLUSION

In this paper, the impact of climate change on hydro-climatological parameters, especially precipitation and temperature, in North Cyprus was evaluated for a period from 2018 to 2040. At a grid point located in Karfas, 13 predictors from BNU-ESM GCM based on CMIP5 under RCP4.5 were used for statistical downscaling and future projection of mean precipitation and temperature over Famagusta, Nicosia, and Kyrenia stations using ANN, ANFIS, and MLR models. MI and CC feature extraction methods were used to determine both nonlinear and linear relationship between the predictors/predictands and, later, the most dominant predictors were used as input variables for the downscaling modeling. The results of the best downscaling model were then used as a benchmark for the future projection of the hydro-climatological parameters.

The results of the feature extraction methods showed that for both precipitation and temperature, different predictors led to different performance. For Famagusta station, based on precipitation, a combination of Huss, Uas, Sfcwind for MI and Psl,

Clwvi, Vas for CC provided the best performance, while Clwvi, Huss, Uas for MI and Tasmax, Huss, Ts led to better accuracy based on temperature. For Nicosia station, based on precipitation, a combination of Huss, Uas, Hurs for MI and Psl, Clwvi, Vas for CC provided the best performance, while Huss, Clwvi, Sfcwind for MI and Tasmax, Huss, Ts led to better accuracy based on temperature. For Kyreniastation, based on precipitation, a combination of Uas, Sfcwind, Psl for MI and Hurs, Ps, Psl for CC provided the best performance, while Uas, Ts, Psl for MI and Tasmax, Huss, Ts led to better accuracy based on temperature. The results of the downscaling modeling showed that the AI-based models performed better than the MLR model. For instance, in terms of precipitation, ANFIS outperformed the other models with 14 and 15% over ANN and MLR, respectively. In terms of temperature, more reliable downscaling was achieved by ANFIS, which has 1.5% and 1.8% higher accuracy than ANN and MLR, respectively. The future projection of the predictands showed a decreasing trend in the annual precipitation and an increasing trend in temperature. This suggests that the greenhouse effect will continue to escalate in the years to come and thus increase global warming with a precipitation decrease of up to 22%, 4.8%, 42% and temperature increase up to 2.9%, 5%, 4.8% for Famagusta, Nicosia, and Kyrenia stations, respectively.

The statistical downscaling models showed better skill for temperature than precipitation. The ensemble model that combines other models shows superior performance in statistical downscaling modeling, such as in the case of Nourani *et al.* (2018) study, therefore, for future studies, the ensemble model should be employed to improve the downscaling performance of precipitation. However, this study employed CMIP5 data to perform the statistical downscaling; with the emergence of CMIP6 data, perhaps more rigorous results could be achieved. It is therefore suggested to use CMIP6 data for future studies and compare.

FUNDING

Not applicable.

CONFLICTS OF INTEREST

The research has no conflict of interest.

CODE AVAILABILITY

The codes are available in the modules of software used.

DATA AVAILABILITY STATEMENT

All relevant data are included in the paper or its Supplementary Information.

REFERENCES

Abdellatif, M., Atherton, W. & Alkhaddar, R. 2013 A hybrid generalised linear and Levenberg–Marquardt artificial neural network approach for downscaling future rainfall in North Western England. *Hydrology Research* **44** (6), 1084–1101.

Abdullahi, J. & Elkiran, G. 2017 Prediction of the future impact of climate change on reference evapotranspiration in Cyprus using artificial neural network. *Procedia Computer Science* **120**, 276–283.

Allen, R. G., Pereira, L. S., Raes, D. & Smith, M. 1998 *Crop Evapotranspiration-Guidelines for Computing Crop Water Requirements*. FAO Irrigation and drainage paper 56. FAO, Rome, Italy, D05109.

Alotaibi, K., Ghumman, A. R., Haider, H., Ghazaw, Y. M. & Shafiquzzaman, M. 2018 Future predictions of rainfall and temperature using GCM and ANN for arid regions: a case study for the Qassim Region, Saudi Arabia. *Water* **10** (9), 1260.

Babel, M. S., Sirisena, T. A. J. G. & Singhrattna, N. 2017 Incorporating large-scale atmospheric variables in long-term seasonal rainfall forecasting using artificial neural networks: an application to the Ping Basin in Thailand. *Hydrology Research* **48** (3), 867–882.

Baghanam, A. H., Nourani, V., Keynejad, M. A., Taghipour, H. & Alami, M. T. 2019 Conjunction of wavelet-entropy and SOM clustering for multi-GCM statistical downscaling. *Hydrology Research* **50** (1), 1–23.

Bowden, G. J., Dandy, G. C. & Maier, H. R. 2005 Input determination for neural network models in water resources applications. Part 1– background and methodology. *Journal of Hydrology* **301** (1–4), 75–92.

Cheng, C. T., Wu, X. Y. & Chau, K. W. 2005 Multiple criteria rainfall–runoff model calibration using a parallel genetic algorithm in a cluster of computers. *Hydrological Sciences Journal* **50** (6), 1069–1088.

Hornik, K., Stinchcombe, M. & White, H. 1989 Multilayer feedforward networks are universal approximators. *Neural Networks* **2** (5), 359–366.

Jang, J. S. 1993 ANFIS: Adaptive-Network-Based Fuzzy Inference System. *IEEE Transactions on Systems, Man, and Cybernetics* **23**, 665–685.

Jang, J. R. & Sun, C. T. 1995 Neuro-fuzzy modeling and control. *Proceedings of the IEEE* **83** (3), 378–406.

Jang, J. S. R., Sun, C. T. & Mizutani, E. 1997 Neuro-fuzzy and soft computing-a computational approach to learning and machine intelligence [Book review]. *IEEE Transactions on Automatic Control* **42** (10), 1482–1484.

Klein, W. H. 1983 Objective specification of monthly mean surface temperature from mean 700 mb heights in winter. *Monthly Weather Review* **111** (4), 674–691.

Landman, W. A., Mason, S. J., Tyson, P. D. & Tennant, W. J. 2001 Statistical downscaling of GCM simulations to streamflow. *Journal of Hydrology* **252** (1–4), 221–236.

Legates, D. R. & McCabe Jr, G. J. 1999 Evaluating the use of 'goodness-of-fit' measures in hydrologic and hydroclimatic model validation. *Water Resources Research* **35** (1), 233–241.

Mora, D. E., Campozano, L., Cisneros, F., Wyseure, G. & Willems, P. 2014 Climate changes of hydrometeorological and hydrological extremes in the Paute basin. *Ecuadorean Andes. Hydrology and Earth System Sciences* **18** (2), 631.

Nourani, V. & Komasi, M. 2013 A geomorphology-based ANFIS model for multi-station modeling of rainfall runoff process. *Journal of Hydrology* **490**, 41–55.

Nourani, V., Khanghah, T. R. & Baghanam, A. H. 2015 Application of entropy concept for input selection of wavelet-ANN based rainfall-runoff modeling. *Journal of Environmental Informatics* **26** (1), 52–70.

Nourani, V., Baghanam, A. H. & Gokcekus, H. 2018 Data-driven ensemble model to statistically downscale rainfall using nonlinear predictor screening approach. *Journal of Hydrology* **565**, 538–551.

Nourani, V., Razzaghzadeh, Z., Baghanam, A. H. & Molajou, A. 2019a ANN-based statistical downscaling of climatic parameters using decision tree predictor screening method. *Theoretical and Applied Climatology* **137** (3–4), 1729–1746.

Nourani, V., Elkiran, G. & Abdullahi, J. 2019b Multi-station artificial intelligence based ensemble modeling of reference evapotranspiration using pan evaporation measurements. *Journal of Hydrology* **577**, 123958.

Nourani, V., Elkiran, G. & Abdullahi, J. 2020 Multi-step ahead modeling of reference evapotranspiration using a multi-model approach. *Journal of Hydrology* **581**, 124434.

Okkan, U. 2015 Assessing the effects of climate change on monthly precipitation: proposing of a downscaling strategy through a case study in Turkey. *KSCE Journal of Civil Engineering* **19** (4), 1150–1156.

Pahlavan, H. A., Zahraie, B., Nasseri, M. & Varnousfaderani, A. M. 2017 Improvement of multiple linear regression method for statistical downscaling of monthly precipitation. *International Journal of Environmental Science and Technology* **15** (9), 1897–1912.

Peng, Y., Zhao, X., Wu, D., Tang, B., Xu, P., Du, X. & Wang, H. 2018 Spatiotemporal variability in extreme precipitation in China from observations and projections. *Water* **10** (8), 1089.

Sahoo, G. B., Ray, C. & Wade, H. F. 2005 Pesticide prediction in ground water in North Carolina domestic wells using artificial neural networks. *Ecological Modelling* **183** (1), 29–46.

Samadi, S., Carbone, G. J., Mahdavi, M., Sharifi, F. & Bihamta, M. R. 2013a Statistical downscaling of river runoff in a semi-arid catchment. *Water Resources Management* **27** (1), 117–136.

Samadi, S., Wilson, C. A. & Moradkhani, H. 2013b Uncertainty analysis of statistical downscaling models using hadley centre coupled model. *Theoretical and Applied Climatology* **114** (3–4), 673–690.

Shannon, C. E. 1948 A mathematical theory of communication. *The Bell System Technical |Journal* **27** (3), 379–423.

Timbal, B., Dufour, A. & McAvaney, B. 2003 An estimate of future climate change for western France using a statistical downscaling technique. *Climate Dynamics* **20** (7–8), 807–823.

Wilson, P. & Mantooth, H. A. 2013 *Model-based Engineering for Complex Electronic Systems*. Newnes, Oxford, UK.

Zorita, E. & Von Storch, H. 1999 The analog method as a simple statistical downscaling technique: comparison with more complicated methods. *Journal of Climate* **12** (8), 2474–2489.